A Giant Step: from Milli- to Micro-arcsecond Astrometry
Proceedings IAU Symposium No. 248, 2007
W. J. Jin, I. Platais & M. A. C. Perryman, eds.

doi:10.1017/S1743921308018966

Astrometry with ALMA: a giant step from 0.1 arcsecond to 0.1 milliarcsecond in the sub-millimeter

J.-F. Lestrade

Observatoire de Paris-CNRS
77 av. Denfert Rochereau, F75014, Paris, France
email: jean-francois.lestrade@obspm.fr

Abstract. We discuss astrometric capabilities of the future interferometer ALMA that will be located at a high altitude site (5000m) in Northern Chile to operate in the sub-millimeter range. In this paper, we estimate the astrometric precision of ALMA to be ~ 0.18 milliarcsecond at the optimum observing frequency of 345 GHz from an error budget including the thermal noise and the systematic errors caused by uncertainties in antenna coordinates, reference source coordinates, Earth orientation parameters, dry atmosphere parameter and by phase fluctuations due to moisture above the site. We briefly discuss three applications: first, astrometric search of exoplanets around 446 nearby stars detectable by ALMA; second, proper motions and parallaxes of pre-stellar cores and protostars; third, the rotation rate of the debris disk around ϵ Eri to test the theory of dust trapping in mean motion resonances with unseen planets.

Keywords. instrumentation: high angular resolution, instrumentation: interferometers, astrometry, submillimeter, circumstellar matter, stars: formation

1. Introduction

ALMA (Atacama Large Millimeter Array) is an international project to build and operate a large millimeter/sub-millimeter interferometer array (up to 80 antennae) at a high altitude site (5000m) in Northern Chile in the Atacama desert. Partners of the project are ESO, US/Canada, Japan and Taiwan. The first concept of the array was the MMA (MilliMeter Array) described in a NRAO memo by Owen (1982). The project began in 2002. Site construction, hardware production lines and software development are now well underway, the first antenna is being installed as of this writing. Early science with a limited operational array is planned for 2010, and full science operations are expected to start in 2012.

ALMA will provide high-angular resolution and high sensitivity images of the molecular Universe and of the cold dust Universe in order to study the origins of planets and stars, and stellar formation in primordial galaxies at high z.

The present array is planned with 54×12-m antennae and 12×7-m antennae placed in different configurations to realise baselines from 150 m, for the most compact array, to 20 km, for the most extended. Ten frequency bands will be covered by the receivers between 31 GHz and 950 GHz. The bandwidth will be 8 GHz with dual polarization. For continuum observations, relevant to astrometry, 1σ flux sensibility will be 0.2mJy in 1 minute of integration time at the optimum frequency of 345 GHz in median atmospheric conditions at Atacama. This sensitivity is unprecedented in the sub-millimeter range.

Several major projects are planned for astrometry in the optical (*e.g.,* Gaia) that will dominate the field in the two decades to come. However, there are intrinsically cold celestial objects that "shine" only at submillimeter wavelengths, for which ALMA will

be the instrument of choice for precise astrometry. Here we present the error analysis to estimate the expected astrometric precision of ALMA and discuss a few astrophysical applications.

2. Astrometric precision of ALMA

Astrometric accuracy depends both on statistical and systematic errors. If there were no systematic errors, *e.g.,* no errors in the station coordinates or in atmospheric pressure, then the theoretical precision of interferometer would be limited by thermal noise only:

$$\sigma_{\alpha,\delta} = \frac{1}{2\pi} \times \frac{1}{SNR} \times \frac{\lambda}{B}. \tag{2.1}$$

Assuming $\lambda = 850\mu$m (345 GHz), SNR=30, B=10 km, $\sigma_{\alpha,\delta}$ would be 0.1 mas. This is unheard of in the sub-millimeter range for astrometry since the existing arrays (IRAM, SMA and CARMA) provide a precision of $\sim$ 0.1 arcsecond. We shall discuss whether or not systematic errors can be controlled to the level that allows us to approach this theoretical precision. To the usual systematic errors encountered in radio interferometry at cm-λ (Thompson, Moran & Swenson (1986)) − uncertainties in the station coordinates, coordinates of reference source, Earth Orientation Parameters, and dry atmosphere zenith delay − rapid phase fluctuations caused by the moisture in the atmosphere – all become critical at sub-millimeter wavelengths. We assume that the ALMA astrometric observations are relative to a reference source that removes long term phase fluctuations from the atmosphere and electronics allowing to expand the integration time to tens of minutes or more as done in VLBI (Lestrade *et al.* (1990)). A typical angular separation between the target and a phase reference source is $\Delta\theta = 6^\circ$, based on the density of strong sources at sub-millimeters (Holdaway *et al.* (2005)).

In our analysis, we use the simplified interferometric formula for the phase: $\phi = f\frac{B\ \sin\theta}{c}$, where θ is the angle between the direction of the source and the normal to the baseline vector, B is the baseline length, f is the effective frequency of observation, c is the speed of light. The differential phase between target and reference sources separated by $\Delta\theta$ is $\Delta\phi \sim f\frac{B\ \cos\theta_0}{c} \times \Delta\theta$, where $\Delta\theta$ is small ($6^\circ/57^\circ \sim 0.1$ radian). Differentiating this equation again − but with respect to baseline B and to reference source position θ_0 this time − yields the error $\delta\Delta\theta$ in the angular separation between these sources that we want to estimate.

Uncertainties in the station coordinates, *i.e.* baseline error δB, cause the error $\delta\Delta\theta \sim \frac{\delta B}{B} \times \Delta\theta$. The ALMA station coordinates can be determined at a level of 50μm after proper calibration of the array, making $\delta B \sim 100\mu$m (Wright (2002) and Conway (2004)). By using $B = 10$ km and $\Delta\theta = 6^\circ$, one gets $\delta\Delta\theta = 0.2$ mas over one baseline. Hence, an array consisting of 66 antennae with uncorrelated coordinate errors yields an overall $\delta\Delta\theta = 0.2/\sqrt{66} = 0.03$ mas for the angular separation between target and reference sources.

Uncertainties of the reference source coordinates $\delta\theta_0$ cause the error $\delta\Delta\theta \sim \delta\theta_0 \times \Delta\theta$. Assuming the precision of absolute positions for the ALMA reference sources to be $\delta\theta_0 = 1$ milliarcsecond – a plausible estimate for ALMA – one gets $\delta\Delta\theta = 0.1$ mas.

Uncertainties in the Earth Orientation Parameters: pole x,y and UT1-UTC are known to a ~ 0.2 mas accuracy as routinely determined by VLBI on daily basis. This uncertainty causes an error similar to $\delta\theta_0$ just mentioned. Thus, $\delta\Delta\theta = 0.02$ mas.

Dry atmosphere : uncertainty of surface pressure. At the elevation E, the path delay through dry atmosphere is given by $\tau = \tau_z/sinE$, with the zenith dry delay τ_z. The elevation E_1 and E_2 at stations 1 and 2 form a small difference $\Delta E = E_2 - E_1 \sim 0.1^\circ$ over

https://doi.org/10.1017/S1743921308018966 Published online by Cambridge University Press

the longest baseline (20 km) for ALMA (unlike to VLBI where $E_1 - E_2$ is usually large). Consequently, the dry atmospheric interferometer phase is $\phi_D = f \times \tau_z \times cosE/sinE^2 \times \Delta E$, where ΔE is small. Thus, the differential dry phase between the target and reference sources is $\Delta\phi_D \sim f \times c\tau_z/c \times \Delta E \times \Delta\theta$, where all angles are in radians and small, and any error $\delta\tau_z$ will produce an error $\delta\Delta\phi_D \sim f \times c\delta\tau_z/c \times \Delta E \times \Delta\theta$. The zenith dry delay τ_z is proportional to the atmospheric pressure. High-quality barometers located at all antennae must be used to calibrate the effect. At Atacama, pressure is about half the pressure at sea level, *i.e.* $c\tau_z$ is $\sim$ 1.15m. Assuming the barometers to be accurate to $\pm$2 millibars, $c\delta\tau_z$ is 5mm and that yields $\delta\Delta\theta \sim 0.02$ mas.

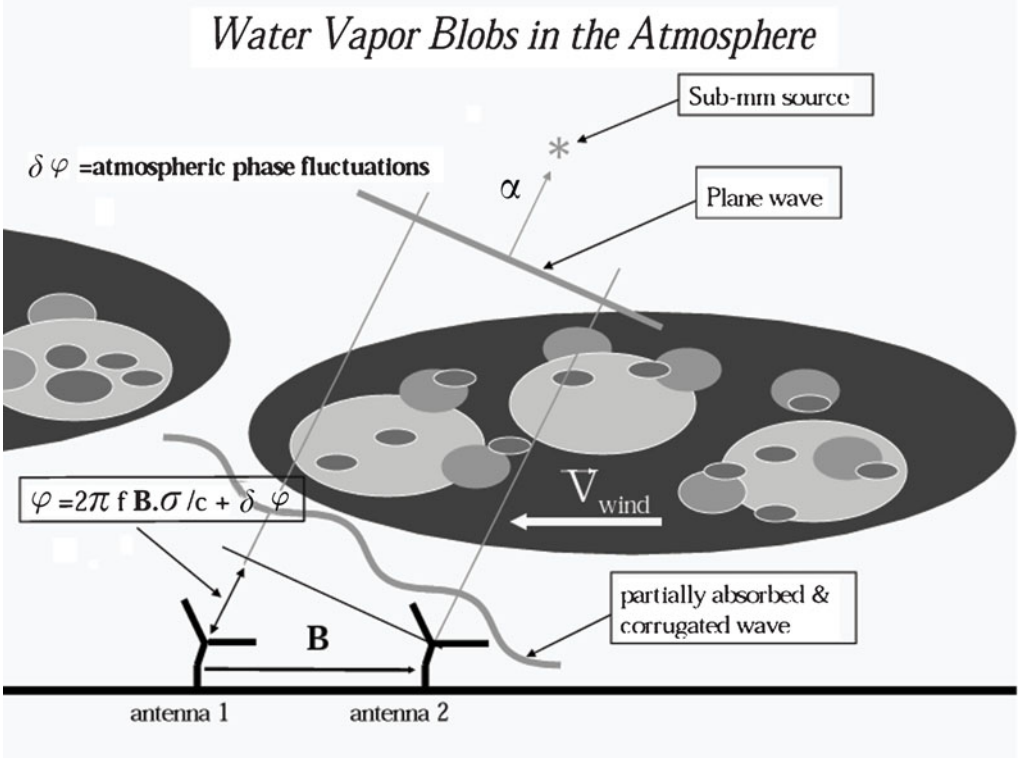

Figure 1. Sketch of the water vapor blobs blown by the wind above ALMA.

Moisture in the atmosphere and phase fluctuations . Fig. 1 shows a sketch of the blobs of water vapor blowing above ALMA. Moisture absorbs millimeter waves and adds fluctuating phase delay to the static dry atmosphere delay. A site as dry as the Atacama desert alleviates this effect but does not make it negligible. In astrometry, absorption impacts only the SNR, and thus the thermal noise of observations (Eq. 2.1). Phase delay fluctuations are more important and should be discussed in some details. These fluctuations have several time scales that depend on the sizes of the water vapor blobs and wind speed over the site. Fluctuations that come from the small blobs have small amplitudes and are rapid ($\sim$1 Hz) for a typical wind speed (10 m/s). Fluctuations that come from the largest blobs (outer scale of the atmosphere) have large amplitudes and are slow ($\sim 10^{-3}$ Hz). The standard approach to quantify fully the atmospheric phase fluctuations is to measure the phase structure function $D_\phi(\rho)$, *i.e.* the phase variance as a function of baseline length ρ. This function is difficult to measure in practice. The best phase structure function above an astronomical site is the one measured for the

https://doi.org/10.1017/S1743921308018966 Published online by Cambridge University Press

VLA at 22 GHz by Carilli & Holdaway (1999) and sketched in Fig 2. Three regimes can be recognized ; for baselines B = 0 to 1.2 km, the phase rms ($\sqrt{D_\phi(\rho)}$) grows as the power-law $B^{0.85\pm0.03}$, characteristic of a turbulent Thick Screen (3-D) ; for baselines B = 1.2 to 6 km, the phase rms grows as $B^{0.41\pm0.03}$, characteristic of a turbulent Thin Screen (2-D) ; and finally for $B > 6$ km, theoretically the phase rms saturates, which is consistent with practice (see Fig. 7 in Carilli & Holdaway (1999)). Saturation of the phase rms occurs when baseline B is long enough to sample the full outer scale of the atmosphere. The two transition baselines between the 3-D and 2-D turbulent regimes (1.2 km on figure) and between the 2-D and saturation regimes (6 km on figure) depend on the site, the frequency, and weather conditions. Needless to say that characterizing a site is demanding. Theory predicts that the outer scale should be the scale height of the atmosphere which is 1-2 km (Pérez-Beaupuits *et al.* (2005)), unlike 6 km found for the VLA.

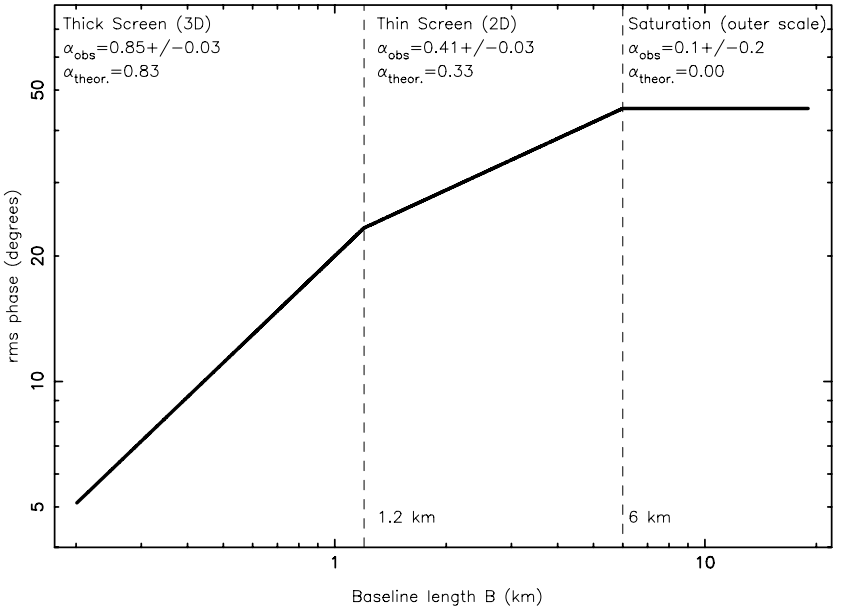

Figure 2. Sketch of the phase structure function measured above the VLA at 22 GHz (in reality, $\phi_{rms} = \sqrt{D_\phi}$ is plotted). Consult Carilli & Holdaway (1999) for the original Fig. 7 inluding data points that allowed to determin α_{obs}.

At the Atacama site, a programme is set up to monitor atmospheric phase fluctuations with an interferometer made of two telescopes, separated by 300 m, to track the carrier of a geostationary satellite at 11.2 GHz since 1995 (Radford *et al.* (1996)). This has allowed to model the phase rms by a power-law : $a \times (\rho/300)^\alpha$, where baseline length ρ is in meters and coefficients a and α are in Table 1 reprinted from Holdaway & Pardo (2001)). The baseline length for which saturation of this function occurs has not been determined yet for Atacama.

Based on this information, the largest phase rms is $\sigma_\phi = 1.86 \times (2000\text{ m}/300\text{ m})^{0.50} \times (345\text{ GHz}/11.2\text{ GHz}) = 148^\circ$ at 345 GHz, in median weather conditions (a=1.86 in Table 1), and assuming an outer scale of 2000 m for the Atacama site. Such phase fluctuations have a time scale of $\sim$ 3 minutes with a wind speed of 10 m s^{-1} (2000 m/10 m s^{-1}). The phase fluctuations can be removed from the data either by monitoring water vapor in the direction of the source by radiometers or by alternating observations between

https://doi.org/10.1017/S1743921308018966 Published online by Cambridge University Press

Table 1. Parameters of the phase structure function $a \times (\rho/300)^{\alpha}$ at the Atacama site from Holdaway & Pardo (2001).

Weather conditions (percentile)	**a** zenith 11.2 GHz (degrees)	α
5% (best)	0.69	0.50
10%	0.91	0.54
20%	1.35	0.56
30%	1.86	0.57
40%	2.46	0.57

the target and reference sources faster than this time scale. A radiometer inverts sky brightness temperature into precipitable water vapor enabling phase fluctuations to be determined. An example of such monitoring between the CSO and JCMT radio telescopes (B = 160 m) at 345 GHz during a normal night at Mauna Kea (precipitable water vapor = 2.6 mm) is provided by Wiedner *et al.* (2001). In their paper, the phase rms is 60° before radiometer corrections, and drops to 26° after corrections (see their Fig. 4).

It is expected that the phase rms can be corrected at least to this level (rms = 26°) on the longest baselines of ALMA because Atacama is drier than Mauna Kea. In the Wiedner *et al.* (2001) phase plot, the uncertainty of the mean phase μ_ϕ is $\sigma_{\mu_\phi} = 26^\circ/\sqrt{180} = 2^\circ$, assuming Gaussian noise for all 180 data points of the corrected phases. This is relevant to astrometry because in the presence of phase fluctuations, a point-like celestial source can be located within the interferometer fringe spacing with a precision of $(\sigma_{\mu_\phi}/2\pi) \times \lambda/B$. Thus, with $\lambda = 850\mu$m (345 GHz) and $B = 10$ km, the mean phase uncertainty σ_{μ_ϕ} of 2° induces an astrometric uncertainty of 0.1 mas. In relative astrometry, this increases to $\delta\Delta\theta = \sqrt{2} \times 0.1$ mas due to the separation uncertainty. Note that this uncertainty is for a single baseline and will scale down as a function of the number of antennae. This functions will depend on the phase fluctuations at all scales ; small scale fluctuations are uncorrelated between antennae, while large scale fluctuations are uncorrelated only if the outer scale of the atmosphere is smaller than the array size. Conservatively, we retain the maximum value $\sqrt{2} \times 0.1$ milliarcsecond for our final error budget.

Table 2. Error budget for ALMA astrometry with a phase reference source separated from the target source by 6°

Error sources	plausible systematic errors	Resulting errors in ALMA α, δ (milliarcsecond)
Ref. Sour. coord.	1 mas	0.1
Station coord.	50μm	0.03
EOP	0.2 mas	0.02
Dry atm. (pressure)	2 millibars	0.02
Moisture (Radiometer)	26° (post-correction rms)	0.14
Thermal noise (SNR)	SNR=30	0.1
Total	all	0.18

Final error budget : Table 2 summarizes the result of our analysis. Combining in quadrature all 6 sources of errors, we estimate the total astrometric precision of ALMA to be $\sim$ 0.18 milliarcsecond, at the optimum observing frequency of 345 GHz, with the

https://doi.org/10.1017/S1743921308018966 Published online by Cambridge University Press

extended configuration, with a target-reference source separation of 6°, and with water vapor monitoring by radiometry. The analytical approach adopted to derive the present error budget for ALMA has been used previously for determining VLBI astrometric errors (Shapiro *et al.* (1979)) that compare satisfactorily to observations (Lestrade *et al.* (1990)) and to numerical simulations (Pradel *et al.* (2006)).

3. Astrometric applications

We explore briefly three possible astrometric applications of ALMA.

3.1. *Search for extra-solar planets*

We have computed the thermal flux densities at 345 GHz for all stars from the CNS3 (Catalogue of Nearby Stars 3rd Edition 1991, by Gliese and Jahreiss), and have found that 446 nearby stars are expected to have flux densities $\geqslant 0.1$ mJy (Table 3) and thus are detectable by ALMA with SNR=30 at reasonable integration time (right-hand plot of Fig. 3). The photospheres of these stars will not be angularly resolved even by the most extended configuration of the array. These are stable sources of emission and can accurately track the reflex motion of unseen planets.

Table 3. Distribution of the CNS3 stars detectable by ALMA above 0.1 milliJansky at 345 GHz. For some stars, the catalogue provides only approximate spectral types that have been interpreted in our analysis as the following : a-f=F0, f=F5, f-g=G0, g=G5, g-k=K0, k=K5, k-m=M0, m=M2, m+=M6.

Spectral Type	Number of stars in the whole CNS3 (mostly d $\leqslant$ 25 pc)	N of stars detectable by ALMA	Fraction of the CNS3
O	0	0	0 %
B	0	0	0 %
A	69	54	78 %
F	266	158	59 %
G	495	125	35 %
K	824	71	9 %
M	1804	36	2 %
Total	3461	446	13 %
Miscellaneous	341		

We have computed also the minimum planetary masses measurable by ALMA over a 10 year long programme and with an astrometric precision of 0.1 mas. The amplitude of the wobble of a central star due to the gravitational pull by planet in a circular orbit is : $\theta = \frac{m}{M}\frac{a}{d} = \frac{m}{d}\left(\frac{P}{M}\right)^{2/3}$ where θ is in arcseconds, a in AU, P in years, d in pc, m and M, the masses of the unseen planet and of the central star, in $M_\odot$. We plot the distribution of planetary masses that ALMA can probe by setting $\theta = 0.1$ mas, $P = 10$ yr, M and d to their values in the CNS3 catalogue, and by solving for m (left-hand plot of Fig. 3). See further details in Lestrade (2003).

3.2. *Pre-stellar cores and Protostars*

Tracing stellar formation phases in star forming regions (*e.g.* ρ Oph cloud at 160 pc) is one of the major current topics in astrophysics. Pre-stellar cores (age from -1 Myr

https://doi.org/10.1017/S1743921308018966 Published online by Cambridge University Press

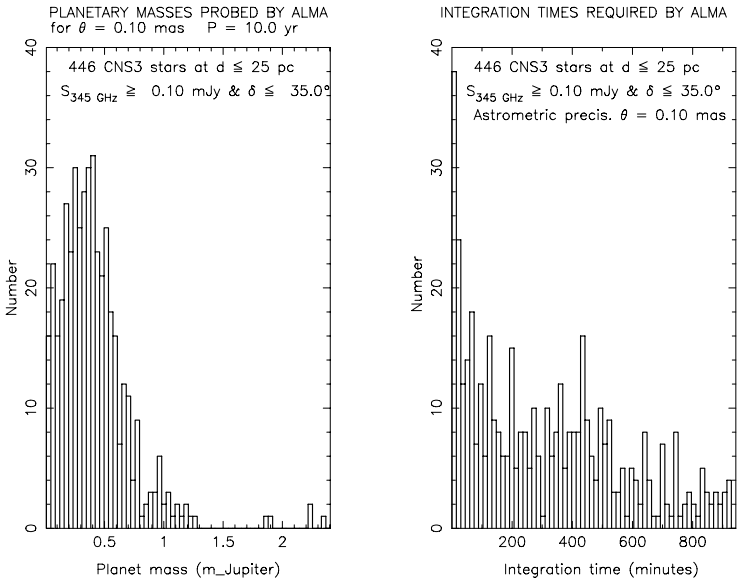

Figure 3. Left: *minimum masses detectable astrometrically by ALMA for possible unseen planets orbiting 446 nearby stars. The corresponding astrometric programme must last at least 10 years and sustain the astrometric precision of 0.1 mas.* **Right:** *the integration time required to reach the theoretical astrometric precision of 0.1 mas by ALMA for the selected 446 stars.*

to 0, stellar birth line), Class 0 protostars (age $\sim 10^4$yr) and Class I protostars (age $\sim 10^5$yr) "shine" only, or mainly, in the sub-millimeter range (André *et al.* (1993)). As suggested by P. André, measurements of proper motions can verify whether or not the rms velocity of pre-stellar cores is <1 km s^{-1} (< 1 mas yr^{-1} at the distance of ρ Oph cloud) while rms velocity of Class 0 and Class I protostars is > 1 km s^{-1} as predicted by theory. This is because pre-stellar cores are still coupled to their original molecular cloud and its magnetic field, while Class 0 and Class I protostars have decoupled, and stellar motions are in virial equilibrium in the gas-mass dominated gravitational potential of the cloud. ALMA with its astrometric precision of proper motions at $\sim$ 0.1 mas yr^{-1} will be able to survey a large sample of these objects to validate this theory. Along with proper motions, trigonometric parallaxes can be produced from such a survey. They will provide the depth of star forming regions.

3.3. *Debris disks*

Stars develop **debris disks** at the end of the planet formation phase when the protoplanetary disk of primordial gas and dust has dissipated. A debris disk is composed of left-over planetesimals (asteroids, comets, Kuiper Belt Objects, Trojans) that could not agglomerate into larger planets during this early phase (< 10 Myrs for solar-mass stars). They are the exosolar analogues of the Kuiper Belt and of the asteroid belt in the Solar System. Collisions between these left-over planetesimals generate dust grains whose large emitting surface make them observable from Mid-IR to sub-mm. The best example of this kind is the disk around a nearby K2V star ϵ Eri imaged by JCMT at 345 GHz (Greaves *et al.* (2005). Their image shows a disk seen almost face-on, and hosting a central cavity. The mean radius of the disk is 60 AU, similar to the Kuiper Belt. The image exhibits a clumpy annular structure that is interpreted as emitting dust grains

https://doi.org/10.1017/S1743921308018966 Published online by Cambridge University Press

trapped into mean motion resonances with an unseen planet orbiting within the central cavity. Simulation of this mechanism permits to find the putative planet by adjusting its orbital parameters in order to achieve a best fit to the image (Wyatt (2003)). If the clumps of the disk structure are compact enough for ALMA, *i.e.* angularly unresolved by the array, astrometric observations can reveal the rotation of the disk which should make all clumps move by ~ 0.5"/yr along directions tangential to a circle (Poulton *et al.* (2006)). With the astrometric precision that we have estimated for ALMA, this can be done with observations between two epochs separated by much less than a year ! The strategy of observations may take advantage of the fact that the photosphere of ϵ Eri can be detected easily by ALMA and used as the reference source. In this case, the proper motion and parallax are common to both the star and its disk, so that they do not bias the measurement of the rotation rate.

References

André, P., Ward-Thompson, D., & Barsony, M., 1993, *ApJ*, 406, 122
Carilli, C. L. & Holdaway, M. A., 1999, *Radio Sc.*, 34, 817
Conway, J., 2004, *Alma Memo Series*, memo#503
Greaves, J. S., *et al.*, 2005, *ApJ*, 619, L187
Holdaway, M. A. & Pardo, J. R., 2001, *Alma Memo Series*, memo#404
Holdaway, M. A., Carilli, C., Weiss, A., & Bertoldi, F., 2005, *Alma Memo Series*, memo#543
Lestrade, J.-F., Rogers, A. E. E., Withney, A. R., *et al.* 1990, *AJ*, 99, 1663
Lestrade, J.-F., 2003, *ASP Conf. Ser.*, 294, 587
Owen, F. N. 1982, *Alma Memo Series*, memo#1
Pérez-Beaupuits, J. P., Rivera, R. C., & Nyman, L.A, 2005, *Alma Memo Series*, memo#542
Poulton, C. J., Greaves, J. S., & Cameron, A. C., 2006, *MNRAS*, 372, 53.
Pradel, N., Charlot, P., & Lestrade, J.-F., 2006, *A&A*, 452, 1099.
Radford, S., Reiland, G., & Shillus, B., 1996, *PASP*, 108, 441
Shapiro, I. I., Wittels, J. J., & Counselman, C. C., 1979, *AJ*, 84, 1459
Thompson, A. R., Moran, J. M., & Swenson, G., 1986, *Interferometry ad Synthesis in Radioastronomy*, publishers : John Wiley & Sons
Wiedner, M. C., Hills, R. E., Carlstrom, J. E., & Lay, O. P., 2001, *ApJ*, 553, 1036.
Wright, M., 2002, *Alma Memo Series*, memo#427
Wyatt, M. C., 2003, *ApJ*, 598, 1321.

https://doi.org/10.1017/S1743921308018966 Published online by Cambridge University Press